

Partial spin freezing in the quasi-two-dimensional $\text{La}_2(\text{Cu},\text{Li})\text{O}_4$

Y. Chen,^{1,2,3} Wei Bao,¹ Y. Qiu,^{2,3} J.E. Lorenzo,⁴ J.L. Sarrao,¹ D.L. Ho,^{2,3} and Min Y. Lin^{2,5}

¹*Condensed Matter and Thermal Physics, Los Alamos National Laboratory, Los Alamos, NM 87545*

²*NIST Center for Neutron Research, National Institute of Standards and Technology, Gaithersburg, MD 20899*

³*Dept. of Materials Science and Engineering, University of Maryland, College Park, MD 20742*

⁴*CNRS, BP 166X, F-38043, Grenoble, France*

⁵*ExxonMobil Research and Engineering Company, Annandale, NJ 08801*

(Dated: November 3, 2018)

In conventional spin glasses, the magnetic interaction is not strongly anisotropic and the entire spin system freezes at low temperature. In $\text{La}_2\text{Cu}_{0.94}\text{Li}_{0.06}\text{O}_4$, for which the in-plane exchange interaction dominates the interplane one, only a fraction of spins with antiferromagnetic correlations extending to neighboring planes become spin-glass. The remaining spins with only in-plane antiferromagnetic correlations remain spin-liquid at low temperature. Such a novel partial spin freezing out of a spin-liquid observed in this cold neutron scattering study is likely due to a delicate balance between disorder and quantum fluctuations in the quasi-two dimensional $S=1/2$ Heisenberg system.

The parent compound for high transition-temperature superconductors, La_2CuO_4 , is an antiferromagnetic (AF) insulator. Magnetic exchange interaction J between the nearest neighbor $S=1/2$ spins of Cu^{2+} ions in the CuO_2 plane is several orders of magnitude stronger than the interplane exchange interaction, making quantum spin fluctuations an essential ingredient for magnetic properties in the quasi-two-dimensional (2D) Heisenberg system[1, 2, 3]. The Néel temperature T_N of La_2CuO_4 is suppressed rapidly by 2–3% hole dopants such as Sr, Ba or Li[4, 5], while it is suppressed with isovalent Cu substitution at a much higher concentration close to the site dilution percolating threshold[6]. The strong effect of holes has been shown to be related to induced magnetic vortices, which are topological defects in 2D systems[7]. The paramagnetic phase exposed by hole doping at $T \ll J/k_B$ is dominated by zero-point quantum spin fluctuations and is referred to as a quantum spin liquid[1]. The approach of the Néel transition toward zero temperature promises detailed predictions for spin dynamics by extending the celebrated theory of critical phenomena for classical statistical systems to quantum statistical systems[1, 8].

However, in a wide doping range of $\text{La}_2\text{Cu}_{1-x}\text{Li}_x\text{O}_4$ below ~ 10 K, a spin-glass transition has been reported in muon spin rotation (μSR)[5], nuclear quadrupole resonance (NQR)[9] and magnetization[10] studies. A similar magnetic phase diagram has also been reported for $\text{La}_{2-x}\text{Sr}_x\text{CuO}_4$ and $\text{Y}_{1-x}\text{Ca}_x\text{Ba}_2\text{Cu}_3\text{O}_6$ [11, 12, 13]. In conventional spin glasses, magnetic interactions are more or less isotropic in space, and the whole spin system is believed to be frozen in the spin-glass phase[14]. If the spin-glass phase in hole-doped cuprates behaved as in conventional spin-glasses, the ground state would be a spin-glass instead of Néel order or quantum spin liquid, and as pointed out by Hasselmann et al.[15], the quantum critical point of the AF phase would be preempted.

Recently, 2D spin fluctuations in $\text{La}_2\text{Cu}_{1-x}\text{Li}_x\text{O}_4$ ($0.04 \leq x \leq 0.1$) were observed to remain liquid-like

below the spin-glass transition temperature T_g [16, 17]. The characteristic energy of 2D spin fluctuations saturates at a finite value below ~ 50 K as expected for a quantum spin liquid[1], instead of becoming zero at T_g as for spin-glass materials[14, 18]. To reconcile these apparently contradicting experimental results, we have conducted a thorough magnetic neutron scattering investigation of $\text{La}_2\text{Cu}_{0.94}\text{Li}_{0.06}\text{O}_4$ to search for spin-glass behavior. We found that in addition to the liquid-like 2D dynamic spin correlations, the rest of spins which participate in almost 3D and quasi-3D correlations become frozen in the spin-glass transition. This partial spin freezing in the laminar cuprate is distinctly different from total spin freezing in conventional 3D spin-glass materials. The observed phase separation into spin glass and spin liquid components of different dimensionality sheds light on a long-standing confusion surrounding the magnetic ground state in hole-doped cuprates.

The same single crystal sample of $\text{La}_2\text{Cu}_{0.94}\text{Li}_{0.06}\text{O}_4$ used previously[16] was investigated in this work. $T_g \approx 8$ K was determined using μSR [5]. The lattice parameters of the orthorhombic $Cmca$ unit cell are $a=5.332\text{\AA}$, $b=13.12\text{\AA}$ and $c=5.402\text{\AA}$ at 15 K. Wave-vector transfers \mathbf{q} near (000) and (100) in both the ($h0l$) and ($hk0$) reciprocal planes were investigated at NIST using the 30 meter high resolution small angle neutron scattering (SANS) instrument at NG7, and cold neutron triple-axis spectrometer SPINS. We set the array detector of NG7-SANS to 1 and 9 m, corresponding to a q range from 0.012 to 0.39 \AA^{-1} and from 0.0033 to 0.050 \AA^{-1} , respectively. At SPINS, the (002) reflection of pyrolytic graphite was used for both the monochromator and analyzer. Horizontal Soller slits of 80' were placed before and after the sample. A cold BeO or Be filter was put before the analyzer to eliminate higher order neutron in the fixed $E_f=3.7$ or 5 meV configuration, respectively. Sample temperature was controlled by a pumped ^4He cryostat which could reach down to 1.5 K.

Hole induced ferromagnetic exchange has been theo-

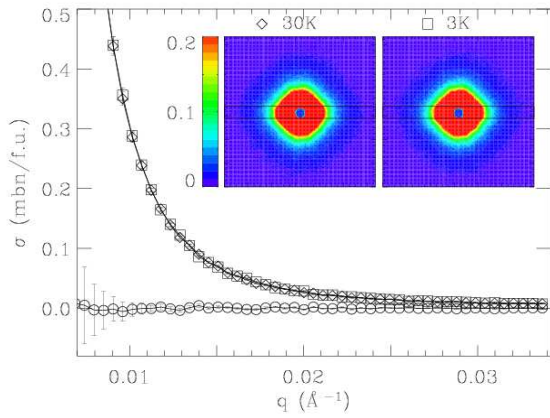


FIG. 1: Measured SANS cross-section in the 10 pixels wide rectangle shown in the inset at 3 K (squares) and 30 K (diamonds), and the difference of the intensity between 3 K and 30 K (circles) as a function of wave vector transfer q . Lines are guide to the eye. Inset: the SANS pattern at 30 and 3 K.

retically proposed in the CuO_2 plane[15, 19]. Although long-range ferromagnetic order has never been observed, there is the possibility of short-range ferromagnetic spin clusters which freeze in the spin-glass state. A powerful tool to probe such clusters is SANS[18]. Two reciprocal zones were studied, with incident beam parallel to the (001) or (010) direction, to cover all spin orientations. The experiments were carried out at 3, 10, 15, 30 and 80 K. A collection time of 1 or 2 hours per temperature provides good statistics. No temperature dependence in the scattering patterns could be detected. The inset to Fig. 1 shows SANS patterns at 3 K and 30 K with incident beam parallel to the (001) direction. Intensity at 3 and 30 K in the rectangular box on the SANS pattern is shown in the main frame. The difference intensity (circles) fluctuates around zero, and its standard deviation sets a upper limit of 1.5×10^{-7} bn or $1.4 \times 10^{-3} \mu_B$ per Cu for ferromagnetic moments in the clusters.

While no appreciable ferromagnetic signal was detected for $\text{La}_2\text{Cu}_{0.94}\text{Li}_{0.06}\text{O}_4$, antiferromagnetic scattering was observed along the rods perpendicular to the CuO_2 plane and intercepting the plane at the commensurate (π, π) -type Bragg points of the square lattice. This means that antiferromagnetic correlations in the CuO_2 plane is chessboard-like, which is simpler than in $\text{La}_{2-x}\text{Sr}_x\text{CuO}_4$ [20]. Elastic and quasielastic scans through such a rod at (100) are shown in Fig. 2(a) at various temperatures. Inelastic scans have been presented in [16]. There is little change in the peak width in these scans, consistent with previous results of temperature independent in-plane correlation length for $\text{La}_2\text{Cu}_{0.95}\text{Li}_{0.05}\text{O}_4$ [2] and $\text{La}_{2-x}\text{Sr}_x\text{CuO}_4$ ($0.02 \leq x \leq 0.04$)[21] below 300 K. Modeling the width of the rod in $\text{La}_2\text{Cu}_{0.94}\text{Li}_{0.06}\text{O}_4$ with Lorentzian

$$\mathcal{L}^\xi(q) = \xi/\pi[1 + (q\xi)^2], \quad (1)$$

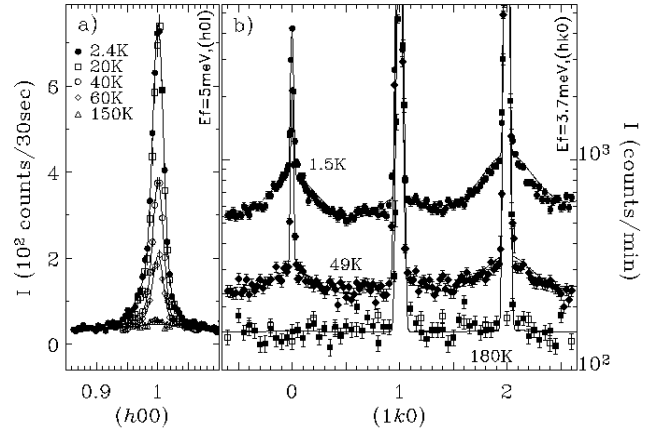


FIG. 2: Magnetic quasielastic and elastic scattering along a) an in-plane direction and b) the interlayer direction at various temperatures. Open squares in b) was measured at $(1.06, k, 0)$ and represent background. The solid lines are resolution convoluted $S^{3D}(\mathbf{q}, E) + S^{q3D}(\mathbf{q}, E)$ in Eq. (3)-(4).

$\xi_{\square}^{3D} \geq 274 \text{ \AA}$ from scan at (100) and $E = 0$, $\xi_{\square}^{q3D} \geq 70 \text{ \AA}$ at $(1, 0.4, 0)$ and $E = 0$, and $\xi_{\square}^{2D} \geq 55 \text{ \AA}$ at finite E from deconvolution. The \square denotes the in-plane component. These planar AF clusters correlate in three different ways in the interlayer direction, giving rise to almost 3D, quasi-3D and 2D magnetic correlations. Let us now examine the three components.

Fig. 2(b) shows elastic and quasielastic scans along the rod in the interlayer direction at 1.5, 49 and 180 K. Magnetic intensity is composed of broad and sharp peaks at magnetic Bragg points (100) and (120) of the parent compound. The (110) peak is temperature-independent thus nonmagnetic. Fitting the broad peaks to Eq. (1), we obtained an interlayer correlation length $\xi^{q3D} = 6.2(4) \text{ \AA}$. Again, no temperature dependence can be detected for ξ^{q3D} below 49 K. Thus, the quasi-3D spin correlations are typically three planes thick. For the sharp peak, $\xi^{3D} \geq 168 \text{ \AA}$. Therefore, the number of correlated AF planes is more than 50, resembling 3D AF order. Both the broad and sharp peaks are energy-resolution-limited with the half-width-at-half-maximum $\leq 0.07 \text{ meV}$, as it is displayed in Fig. 3 and in [16]. However, they should not be regarded automatically as from *static* magnetic order. Static magnetic signal was observed in μSR study[5] only below $T_g = 8 \text{ K}$ at the spin glass transition. Thus, the energy spectra for the quasi-3D and almost 3D correlations may be modeled by $\mathcal{L}^{1/\epsilon}(E)$, with ϵ/h much smaller than $17 \text{ GHz} = 0.07 \text{ meV}/h$, the frequency resolution at SPINS, and larger than the zero-field μSR static cutoff frequency of about 1 MHz [5, 12] for $T > 8 \text{ K}$.

The 2D AF correlations have been investigated in detail in [16]. The dynamic magnetic structure factor,

$$S^{2D}(\mathbf{q}, E) = \sum_{\tau} \mathcal{L}^{\xi_{\square}^{2D}}(\kappa_{\square}) \frac{\chi''(E)}{\pi(1 - e^{-\hbar\omega/k_B T})}, \quad (2)$$

has been measured for $E \leq 4.2 \text{ meV}$ between 1.5 and

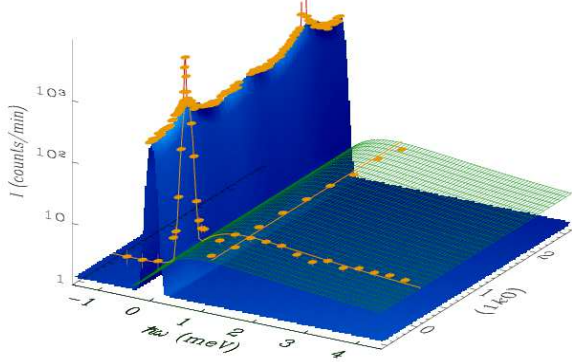


FIG. 3: Measured $S(\mathbf{q}, E)$ as a function of E and interlayer k at 1.5 K, showing three color-coded magnetic components in Eq. (5). The $E = 0$ peak is energy-resolution limited.

150 K near a magnetic Bragg wave-vector τ , and $\kappa \equiv \mathbf{q} - \tau$. The almost 3D and quasi-3D spin correlations can be described, respectively, by

$$S^{3D}(\mathbf{q}, E) = I^{3D} \sum_{\tau} \mathcal{L}^{\xi_{\square}^{3D}}(\kappa_{\square}) \mathcal{L}^{\xi_{3D}}(k - \tau_k) \mathcal{L}^{1/\epsilon}(E) \quad (3)$$

and

$$S^{q3D}(\mathbf{q}, E) = I^{q3D} \sum_{\tau} \mathcal{L}^{\xi_{\square}^{q3D}}(\kappa_{\square}) \mathcal{L}^{\xi_{q3D}}(k - \tau_k) \mathcal{L}^{1/\epsilon}(E). \quad (4)$$

With negligible ferromagnetic correlations, the total dynamic structure factor is a summation of Eq. (2)-(4),

$$S(\mathbf{q}, E) = S^{2D}(\mathbf{q}, E) + S^{q3D}(\mathbf{q}, E) + S^{3D}(\mathbf{q}, E). \quad (5)$$

Of the four variables of $S(\mathbf{q}, E)$, \mathbf{q}_{\square} is fixed at the (π, π) -type Bragg points. To comprehend the composition of $S(\mathbf{q}, E)$, it is sufficient to plot $S(\mathbf{q}, E)$ as a function of E and the interlayer wavenumber k . Such a plot of measured $S(\mathbf{q}, E)$ at 1.5 K is shown in Fig. 3, with the temperature and \mathbf{q} independent incoherent scattering at $E = 0$ subtracted. The sharp peak fitted by the red curve is from $S^{3D}(\mathbf{q}, E)$, the narrow blue ridge at $E=0$ from $S^{q3D}(\mathbf{q}, E)$, and the green surface from $S^{2D}(\mathbf{q}, E)$. The red peak at (100) is about one/three orders of magnitude stronger than the peak intensity of the blue/green surface, respectively.

The spectral weights $\int d\mathbf{q}dE S^{3D}(\mathbf{q}, E) = I^{3D}$ and $\int d\mathbf{q}dE S^{q3D}(\mathbf{q}, E) = I^{q3D}$ can be obtained by fitting resolution-convoluted Eq. (3)-(4) to scans in Fig. 2(b). They are shown as a function of temperature in Fig. 4 with I^{3D} magnified by a factor of 5 for clarity. For the 2D component,

$$I^{2D} = \int dE \frac{2\chi''(E)}{\pi(1 - e^{-\hbar\omega/k_B T})}. \quad (6)$$

Green circles in Fig. 4 represent I^{2D} with energy integration from -0.5 to 4.2 meV, the same interval as in

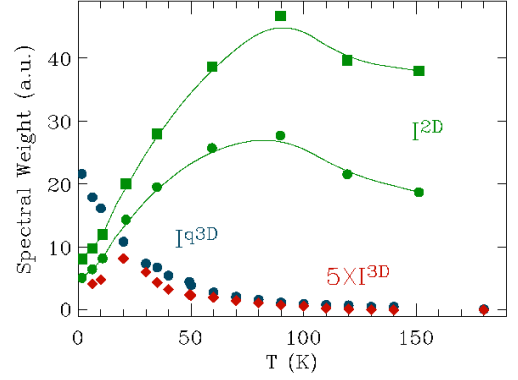


FIG. 4: Temperature dependence of spectral weights I^{2D} (green), I^{q3D} (blue) and I^{3D} (red). See text for details.

experiment[16]. Green squares are obtained with a wider integration range, $|E| \leq 10$ meV, using the analytical expression of $\chi''(E)$ in [16] to extrapolate to $E=10$ meV, where spin fluctuations were observed in $\text{La}_2\text{Cu}_{0.9}\text{Li}_{0.1}\text{O}_4$ using a thermal neutron spectrometer[22]. Thus, the green symbols serve as the lower bound of the 2D spectral weight which has $\pm\infty$ as the integration limits.

I^{3D} and I^{q3D} appear simultaneously below ~ 150 K. Their concave shape in Fig. 4 differ drastically from the usual convex-shape of a squared order parameter, which was observed in μSR study below $T_g=8$ K[5]. They are typical neutron scattering signal from slow *dynamic* spin correlations in spin-glasses[18, 23], which fluctuate in the frequency window between 1 MHz and 17 GHz for $T > 8$ K, and below 1 MHz for $T < 8$ K. Previously, energy-resolution-limited neutron scattering from $\text{La}_{1.94}\text{Sr}_{0.06}\text{CuO}_4$ was observed to have a similar temperature dependence as I^{3D} in Fig. 4 and was attributed to spin freezing[12]. The kink at 20 K of I^{3D} reflects an increased T_g from 8 K to 20 K when probing frequency is increased from 1 MHz to 17 GHz[12, 14].

The fact that I^{3D} decreases below $T_g(17\text{MHz}) \approx 20$ K while I^{q3D} continues to increase indicates that the “Edwards-Anderson order parameter” [14, 18, 23] distributes only along the $(1k0)$ line. In conventional spin-glasses, the “Edwards-Anderson order parameter” is more isotropically distributed in the \mathbf{q} -space[14, 18, 23]. Thus, the spin-glass state in $\text{La}_2\text{Cu}_{0.94}\text{Li}_{0.06}\text{O}_4$ is characterized by interlayer disorder which upsets phase correlation between large AF clusters in different CuO_2 planes. Another important difference from conventional spin-glasses in which all spins freeze below T_g is that only a fraction of spins freeze in $\text{La}_2\text{Cu}_{0.94}\text{Li}_{0.06}\text{O}_4$. Other spins in 2D correlations remain fluctuating down to 1.5 K. This is consistent with previous theory that quantum fluctuations prevent spin-glass transition for 2D $S=1/2$ Heisenberg system[24]. The spin-glass component in our sample has to acquire interlayer correlations to achieve a higher dimension in order to be realized. It appears that the

lower critical dimension for a $S=1/2$ Heisenberg quantum spin glass is between 2 and 3. A further difference from conventional spin-glasses, for which one can measure the narrowing of magnetic spectrum toward $E=0$ [18], is that when $S^{3D}(\mathbf{q}, E)$ and $S^{q3D}(\mathbf{q}, E)$ in $\text{La}_2\text{Cu}_{0.94}\text{Li}_{0.06}\text{O}_4$ become detectable at about 150 K, they are already energy-resolution-limited. This property of $S^{3D}(\mathbf{q}, E)$ and $S^{q3D}(\mathbf{q}, E)$ resembles the classic central peak phenomenon in the soft phonon transition[25]. The disparate dynamics of the central peak and phonon are explained by Halperin and Varma[26] using a phase separation model: defect cells contribute to the slow relaxing central peak while coherent lattice motions (phonons) to the resolved inelastic channel. This mechanism has been applied with success to a wide class of disordered relaxor ferroelectrics[27, 28].

For $\text{La}_2\text{Cu}_{0.94}\text{Li}_{0.06}\text{O}_4$, we envision that disorder accompanying doping prevents the long-range order of the AF phase mainly by upsetting interlayer magnetic phase coherence, see Fig. 3 for the \mathbf{q} -distribution of frozen spins. This upsetting is not uniform in the Griffiths fashion[29] with weak and strong coupling parts in the sample. In our laminar material, however, the weak and strong coupling parts have different dimensionality: 2D and nearly 3D, respectively. The 2D part is a spin liquid and represents essentially the whole system at high temperature, see Fig. 4. Part of sample with stronger interplane coupling tends to order three dimensionally below ~ 150 K, producing $S^{3D}(\mathbf{q}, E)$ and $S^{q3D}(\mathbf{q}, E)$. The condensation of the 2D spin liquid at ~ 150 K into the 3D dynamic clusters of diminishing energy scale, instead of a true long-range order, may reflect the divergent fluctuations which destabilize static order below the critical temperature for random XY or Heisenberg systems[30]. The nearly 3D spin-glass instead of a 3D antiferromagnet finally orders at a much reduced $T_g \approx 20$ K, when $I^{q3D} + I^{3D}$ approaches the 2D spectral weight (Fig. 4). The phase separation into spin liquid and spin glass components may be a consequence of no true mobility edge separating finite and infinite range correlations at 2D[30]. It would be interesting to extend the nonrandom theories[1] to incorporate this disorder scenario and to explain the observed crossover from the E/T to a constant E scaling in the 2D spin liquid[16, 17].

In summary, spins in $\text{La}_2\text{Cu}_{0.94}\text{Li}_{0.06}\text{O}_4$ develop *dynamic* AF order in the CuO_2 plane with very long ξ_{\square} below 150 K. The characteristic energy of the 2D spin fluctuations is $0.18k_B T$ for $T > 50$ K and 1 meV for $T < 50$ K[16]. Below ~ 150 K, interlayer phase coherence appears between some of these planar AF clusters with an energy scale smaller than $70 \mu\text{eV}$. While the 2D AF correlations in an individual plane remain liquid down to 1.5 K, coherent multiplane AF correlations become glassy below T_g . The phase separation into 2D spin-liquid and

“3D” spin-glass is most likely related to quasi-2D nature of magnetic exchange in the cuprates and is distinctly different from conventional spin-glasses. The theory of the spin-glass phase in doped cuprates should consider interlayer coupling, despite it is weak. Investigation of disorder effect on quantum critical spin fluctuations is called for. The phase separation, instead of a uniform magnetic phase, suggests a possibility that superconductivity and the almost 3D AF order reside in different phases in $\text{La}_{2-x}\text{Sr}_x\text{CuO}_4$ and $\text{Y}_{1-x}\text{Ca}_x\text{Ba}_2\text{Cu}_3\text{O}_{6+y}$.

We thank R.H. Heffner, S.M. Shapiro and L. Yu for useful discussions. SPINS and NG7-SANS are supported partially by NSF. Work at LANL is supported by DOE.

-
- [1] S. Chakravarty et al., Phys. Rev. Lett. **60**, 1057 (1988); S. Sachdev and J. Ye, *ibid* **69**, 2411 (1992).
 - [2] Y. Endoh et al., Phys. Rev. B **37**, 7443 (1988).
 - [3] S. M. Hayden et al., Phys. Rev. Lett. **67**, 3622 (1991).
 - [4] T. Nagano et al., Phys. Rev. B **48**, 9689 (1993).
 - [5] R. H. Heffner et al., Physica B **312**, 65 (2002).
 - [6] M. Hücker et al., Phys. Rev. B **59**, R725 (1999).
 - [7] S. Haas et al., Phys. Rev. Lett. **77**, 3021 (1996); C. Timm and K. H. Bennemann, *ibid* **84**, 4994 (2000).
 - [8] J. A. Hertz, Phys. Rev. B **14**, 1165 (1976); A. J. Millis, *ibid* **48**, 7183 (1993).
 - [9] B. J. Suh et al., Phys. Rev. Lett. **81**, 2791 (1998).
 - [10] T. Sasagawa et al., Phys. Rev. B **66**, 184512 (2002).
 - [11] D. R. Harshman et al., Phys. Rev. B **38**, 852 (1988).
 - [12] B. J. Sternlieb et al., Phys. Rev. B **41**, 8866 (1990).
 - [13] F. C. Chou et al., Phys. Rev. Lett. **71**, 2323 (1993); *ibid* **75**, 2204 (1995); C. Niedermayer et al., Phys. Rev. Lett. **80**, 3843 (1998).
 - [14] K. Binder and A. P. Young, Rev. Mod. Phys. **58**, 801 (1986).
 - [15] N. Hasselmann et al., Phys. Rev. B **69**, 014424 (2004).
 - [16] W. Bao et al., Phys. Rev. Lett. **91**, 127005 (2003).
 - [17] Y. Chen et al., (2004), cond-mat/0408547.
 - [18] K. Motoya et al., Phys. Rev. B **28**, 6183 (1983).
 - [19] R. J. Gooding et al., Phys. Rev. B **55**, 6360 (1997).
 - [20] M. Fujita, et al., Phys. Rev. B **65**, 64505 (2002).
 - [21] B. Keimer et al., Phys. Rev. B **46**, 14034 (1992).
 - [22] W. Bao et al., Phys. Rev. Lett. **84**, 3978 (2000).
 - [23] A. P. Murani and A. Heidemann, Phys. Rev. Lett. **41**, 1402 (1978).
 - [24] R. N. Bhatt and P. A. Lee, Phys. Rev. Lett. **48**, 344 (1982).
 - [25] S. Shapiro et al., Phys. Rev. B **6**, 4332 (1972); T. Riste et al., Solid State Comm. **9**, 1455 (1971).
 - [26] B. I. Halperin and C. M. Varma, Phys. Rev. B **14**, 4030 (1976).
 - [27] E. Courtens, J. Phys. (Paris) **43**, L199 (1982).
 - [28] G. Burns and F.H. Dacol, Phys. Rev. B **28**, 2527 (1983).
 - [29] H. Rieger and A. P. Young, in *Complex Behaviour of Glassy Systems*, edited by J. M. Rubí and C. Pérez-Vicente (Springer, Berlin, 1997), p. 256.
 - [30] J.A. Hertz et al., Phys. Rev. Lett. **43**, 942 (1979).